

Secondary-beam intensities

Choice of primary-beam energy and target thickness

The optimum values for target thickness and incident-beam energy are chosen according to the following arguments:

- The optimum target thickness d_{opt} gives a maximum rate for nuclei close to the projectile at the exit of the target. The value of d_{opt} is almost independent of the beam energy, if the range of the projectiles is larger than the optimum target thickness.
- The optimum beam energy is chosen by the condition that the range of the projectile is 3 times the optimum target thickness in order to assure a relatively small emittance of the secondary beam.

Figure 1 illustrates that primary-beam energies in the order of 1 to 1.5 A GeV are required for optimum conditions. Additional arguments for these high primary-beam energies arise from the ionic charge-state distribution and from the kinematic forward focussing of the reaction products that ensure a good separation quality and a high efficiency in the isotopic separation, respectively. For special applications, these high-energetic secondary beams (1.2 to 1.5 A GeV) can even be stopped with only moderate losses in a thick tantalum stopper (See lower part of Fig. 1).

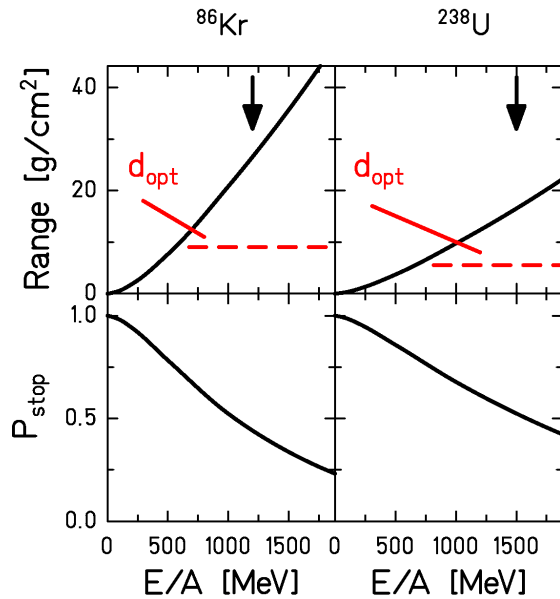


Fig. 1: Quantities relevant for the choice of the primary-beam energy in an in-flight facility. Upper part: Ranges of ^{86}Kr (left) and ^{238}U (right) in the carbon production target. Additionally, the "optimum" target thickness d_{opt} is shown for comparison which gives maximum production. The arrows indicate the optimum energies, 1.2 A GeV for ^{86}Kr and 1.5 A GeV for ^{238}U which assure a good secondary-beam quality. (See text for details.) Lower part: Probability P_{stop} for stopping projectile fragments close to the projectile in a tantalum stopper without nuclear reactions.

Characteristics of the reaction mechanisms

At SIS200 energies, the reaction mechanisms are governed by individual nucleon-nucleon interactions. These interactions can well be represented by the intra-nuclear cascade model or, in the case of heavy-ion collisions, also by the abrasion model. The reaction partner of interest will partly survive as a spectator with a number of nucleons being ejected. The variation of binding energies of protons and neutrons as a function of neutron excess has almost no influence on this reaction step. Therefore, the intermediate products arising from high-energy collisions show a very important fluctuation in the N/Z degree of freedom corresponding directly to the statistics of the nucleon-nucleon collisions.

These intermediate products form a thermalised excited nucleus. The excitation energy may reach values of a few hundred MeV and higher for relativistic heavy-ion collisions. The excited nuclei emit nucleons and light clusters. Another possible decay process during the evaporation cascade is nuclear fission. If the evaporation chain is long enough, the final residues are situated on a characteristic and rather universal ridge on the chart of the nuclides, situated between the proton drip-line and the valley of beta stability. Fission in any stage of the de-excitation process populates more or less neutron-rich fragments in the mid-mass region with rather important fluctuations in mass and quite limited fluctuations in neutron excess.

These considerations have been verified by comparison with experimental data. In particular, a systematic study of the production of heavy residual nuclei in reactions at relativistic energies has been performed at GSI in several recent experiments in inverse kinematics, e.g. [1, 2, 3, 4]. They cover projectiles from ^{129}Xe to ^{238}U in combination with target nuclei ranging from hydrogen to lead. These experiments allow for the first time to obtain a complete overview on the isotopic production cross sections in relativistic nuclear collisions. On the basis of these data, realistic parameters for model calculations can be deduced in order to improve the predictive power of these models. Two kinds of models were developed for predictions of production cross sections, the semi-empirical systematics EPAX [5], applicable for limiting fragmentation, and ABRABLA [6], a modern version of the abrasion-ablation model with a careful description of fission included [7].

Figure 2 illustrates in a few examples the complexity of relativistic heavy-ion collisions and the experimental knowledge acquired at GSI. For a global orientation, the cluster plot shows the production cross sections above 10 μb from the reaction ^{238}U on ^{208}Pb at 1 A GeV [3]. A few selected dedicated studies for isotopes of nickel and tin as well as for isotones with $N=118$ which reach down below the nb level are shown in addition. The isotopic distributions resulting from the different reactions show very specific characteristics. Fragmentation leads to increasing mass loss when the energy deposit increases due to more central collisions. Fission products of ^{238}U reach far to the neutron-rich side. A very specific contribution of low-energy fission, characterised by shell effects in the fragments, is observed in electromagnetic-induced fission from $^{238}\text{U} + ^{208}\text{Pb}$. These data form a reliable basis for adjusting the parameters and verifying the predictions of the model calculations in order to allow for realistic predictions. The data shown in the insets are almost perfectly reproduced by the models. The small discontinuity between calculated and measured yields at $Z=28$ in $^{238}\text{U} + ^{208}\text{Pb}$ is not crucial for the predictions presented in the next sections, because the highest yields are obtained if the mass loss is kept small by choosing an appropriate projectile.

Quantitative predictions

Secondary-beam intensities of the proposed facility were estimated under the following conditions. Carbon was used as production target. The semi-empirical systematics EPAX was used for calculating fragmentation cross sections of all primordial nuclides up to ^{209}Bi used as primary beams. The production of projectile fragments and fission residues from the fissile projectile ^{238}U was calculated with the ABRABLA code. Primary-beam intensities ranging from 1×10^{12} per second for ^{238}U to 3×10^{12} per second for ^{20}Ne were used. The optimum target thickness was always used (see Fig. 1). The predicted rates are depicted in Fig. 3 on a chart of the nuclides and for some isotopic chains.

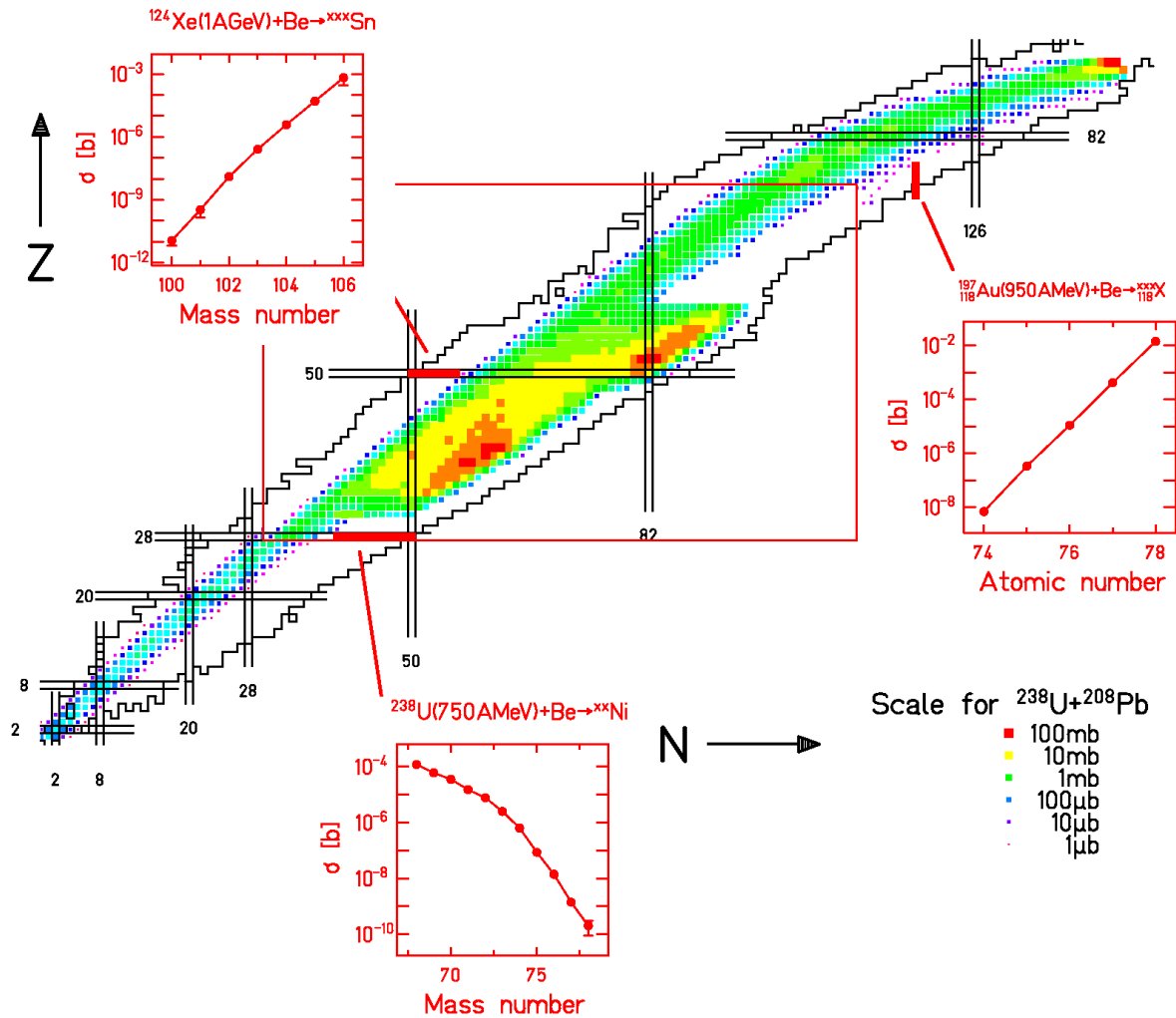


Fig. 2: Illustration of the characteristics of the residue production in relativistic heavy-ion collisions. The clusters in the rectangular box represent yields measured for the reaction $^{238}\text{U} + ^{208}\text{Pb}$ at 1 A GeV. For $Z < 28$ and for $Z > 75$, the data are completed by calculations with the EPAX and ABRABLA codes, respectively. The insets show production cross sections obtained for other reactions in specific experiments, exploring the production far from beta stability in asymmetric fission (neutron-rich nickel isotopes), in hot (tin isotopes) and cold ($N=118$ isotones) fragmentation, respectively.

The estimates are aimed for experiments with the slow-extraction mode and without isotopic separation. The eventual use of profiled energy degraders might induce losses up to 50

% due to nuclear reactions occurring in the degrader. Similar losses are expected when stopping the secondary beam for special applications.

The possibilities to obtain higher intensities of extremely exotic nuclides by two-step reactions have carefully been studied. Considerable gain factors predicted by EPAX turned out to be extremely doubtful when compared with the results of the ABRABLA code which considers the influence of neutron excess on the production cross sections in a more realistic way [8]. Therefore, two-step reactions are not included in the predictions. This explains considerable differences with respect to predictions made elsewhere [9].

In addition to all known nuclides up to ^{238}U , a large number of nuclides beyond the actual limits will become accessible. The most important progress is to be expected in the neutron-rich region above the fission fragments, where the $N=126$ and the $Z=82$ shell can be followed over a long chain of isotones and isotopes, respectively. In particular, the r-process path in the vicinity of the $N=126$ shell comes into reach.

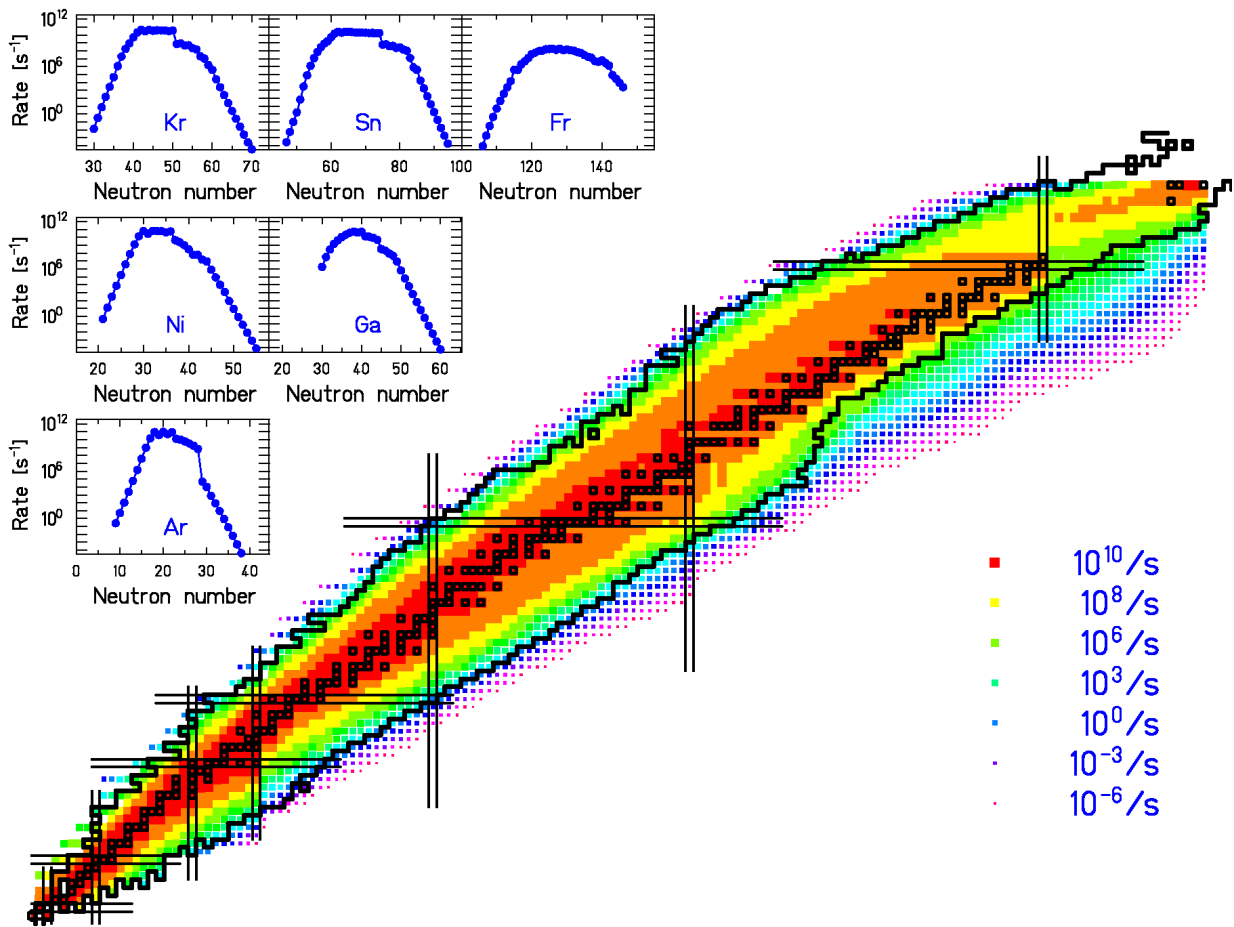


Fig. 3: Predicted secondary-beam intensities for the proposed facility. Values are given only for nuclei with half-lives estimated to be longer than 100 ns. Primordial nuclei and the limits of the actually known nuclides are indicated. The insets show the predictions for the isotopic chains of a few selected elements.

-
- [1] C. Engelmann et al., Z. Phys. A 352 (1995) 351
 - [2] J. Reinhold et al., Phys. Rev. C 58 (1998) 247
 - [3] T. Enqvist et al., Nucl. Phys. A 658 (1999) 47
 - [4] J. Benlliure et al., Nucl. Phys. A 660 (1999) 87
 - [5] K. Sümmerer, B. Blank, Phys. Rev. C 61 (2000) 034607
 - [6] J.-J. Gaimard, K.-H. Schmidt, Nucl. Phys. A 531 (1991) 709

-
- [7] J. Benlliure et al., Nucl. Phys. A 628 (1998) 458
 - [8] J. Benlliure et al., GSI Preprint 2000-41
 - [9] Estimated yields expected for RIA (<http://www.phy.anl.gov/ria/index.html>)